BENTHAM SCIENCE

CrossMark

Current Medical Imaging

Content list available at: https://benthamscience.com/journals/cmir

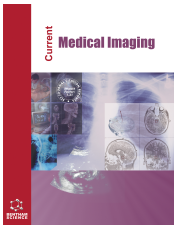

RESEARCH ARTICLE

Correlation of Diffusion weighted MR Imaging and ADC Values of Hepatic Metastasis of Gastrointestinal Stromal and Gastroenteropancreatic Neuroendocrine Tumors

Hasan Aydın[1,*], Melike Ruşen Metin[2] and Volkan Kızılgöz[3]

[1]*Department of Radiology, Ankara Oncology Research hospital, Demetevler, Yenimahalle, Ankara, Turkey*
[2]*Department of Radiology, İstanbul Medipol University, Pendik Education and Research Hospital, Adnan Menderes Bulvarı, Bahçelievler Mah. No:31/33 Pendik, İstanbul*
[3]*Department of Radiology, Binali Yildirim University, Erzincan, Turkey*

Abstract:

Background:

DWI and ADC-mapping was performed to analyze hepatic metastasis of GIST, GEP-NET.

Objective:

The objective of this study is to present hepatic metastasis of GIST and GEP-NET with Diffusion weighted MR imaging(DWI) and the Apparent diffusion coefficients (ADC) values of masses.

Methods:

18 GIST patients and 8 GEP-NET patients were examined retrospectively. 11 males and 6 females were present in GIST group, 7 males to 5 females were involved in GEP-NET group. 18 primary GIST and 10 hepatic metastasis of GIST, 8 original GEP-NET and 19 hepatic metastasis of GEP-NET; total 55 GIST and GEP-NET masses were analysed by ADC mapping. MR images were acquired by 1,5 T MR units (32 mT/min gradient strength- Achieva; Philips Healthcare, Best, Netherlands and 32 channel GE Signa GE-Wisconsin-USA); by using a 4-8 channel standard phased-array torso XL coil, all images were evaluated by an Abdominal MRI experienced radiologist. DWI was performed in the transverse plane by using spin-echo-planar imaging sequence.

Results:

No statistical differences were observed between GIST and GEP-NET patients according to age and gender variations. No significant statistical differences were observed according to the diameters and ADC values of GIST and GEP-NET patients. A significant statistical difference was observed between GIST and GEP-NET groups in terms of size of liver metastasis which was significantly higher in GIST patients. All three groups (GIST_Hep. MET, GEP-NET_Liver_Met and normal) were statistically differed according to ADC values. With the ROC curve analysis: Hepatic metastasis of GIST(n=10) and normal liver (n:47) had cut-off value for ADC: 0.925 under AUC: 0.939 with regard to ADC values and regarded 89.4% Sensitivity, 100% Specificity, 100% PPV and 66.7% PPV. ROC curve of GEP NET_ Hepatic metastasis (n=19) group and normal liver (n:47) group presented cut-off value for ADC: 0.860 under AUC: 0.967 correlated to ADC values with 93.6% sensitivity, 89.5% specificity, 95.7% PPV and 85% PPV.

Conclusion:

High cellular tumors resulted from liver metastasis of GIST and GEP-NET's, and a positive correlation was observed between ADC values and cellularity/differentiation ratios of metastatic masses.

Keywords: MR, Imaging, Diffusion, Hepatic, Metastasis, GIST.

Article History	Received: October 01, 2022	Revised: March 22, 2023	Accepted: April 12, 2023

1. INTRODUCTION

Gastrointestinal stromal tumors (GIST's) are extremely rare, and constitute 0.1-3% of all gastrointestinal tumors and 5-7% of all sarcomas [1, 2]. They typically originate from bowel wall, muscularis propria or from the muscularis mucosa or between those layers, generally result from Cajal cells within the bowel wall [1 - 5]. 70-80% of GIST's are benign, 20-30% of them are malignant: Benign tumors are common in the stomach, mostly exceeding 5 cm in diameter, have irregular surface and margins with metastatic potentials and heterogeneous contrast enhancement patterns in CT and MRI whereas malignant ones mostly originate from the small intestine [3 - 7].

Neuroendocrine tumors (NET) are heterogeneous neoplasms arising from the secretory cells of a diffuse neuroendocrine system, and they are characterized by an indolent growth rate and the ability to secrete a variety of peptide hormones and biogenic amines [8 - 12]. Gastroenteropancreatic NET's (GEP-NET) include carcinoid tumors of the gastrointestinal tract and pancreatic NET(pNET), whereas carcinoid tumors originate from enterochromaffin cells of the gut, pNET's are believed to arise from the islets of Langerhans, although an alternative origin exists from precursors in the ductal epithelium, has been hypothesized [13 - 17].

GEP-NET's may present themselves as hormonally functioning or nonfunctioning tumors and may have distinct clinical features based on their site of origin [9, 11, 14]. The clinical aggressiveness of NET's can vary based on the primary site; NET's of the small intestine have relatively high malignant potential but tend to progress indolently in the metastatic setting. Conversely, gastric and rectal NET's often have a low tendency to metastasize but can progress rapidly once they become metastatic [9, 14 - 16]. pNET's are usually hormonally silent but may produce a variety of peptide hormones, including insulin, gastrin, and glucagon, thus causing the respective clinical syndromes (insulinoma syndrome, gastrinoma syndrome, glucagonoma syndrome, *etc.*) [9, 13, 16, 17].

The main aim of this research is to present hepatic metastasis of GIST's and GEP-NET's with Diffusion weighted MR imaging(DWI) and the Apparent diffusion coefficients (ADC) values of masses, also utilize the relationship of the cellularity/differentiation ratios of these metastatic masses.

2. MATERIALS AND METHODS

We evaluated 18 GIST patients and 8 GEP-NET patients retrospectively, all these 26 patients were diagnosed between 2013-2020. Mean age of GIST patients was 57.18 ± 12.98, and GEP-NET patients were 57.50 ± 15.52 (Table **1**). 11 males and 6 females were present in GIST group, 7 males to 5 females were involved in GEP-NET group.

18 primary GIST and 10 hepatic metastasis of GIST, 8 original GEP-NET and 19 hepatic metastasis of GEP-NET; total 55 GIST and GEP-NET masses were analysed by ADC mapping (Figs. **1** - **5**). Pixel-based ADC maps were reconstructed with commercially available workstation. ADC values of the detected masses were measured by using an average 10-20 mm diameter region of interest(ROI) at b =800 sec/mm^2 and an average of three measures were handled as the main ADC value (Tables **2** and **3**).

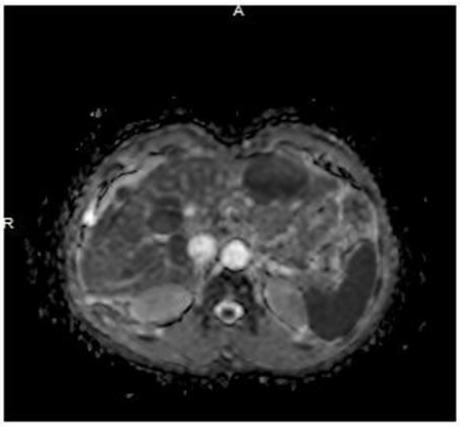

Fig. (1). Multiple hepatic metastasis of a GEP-NET with very low ADC values in ADC mapping.

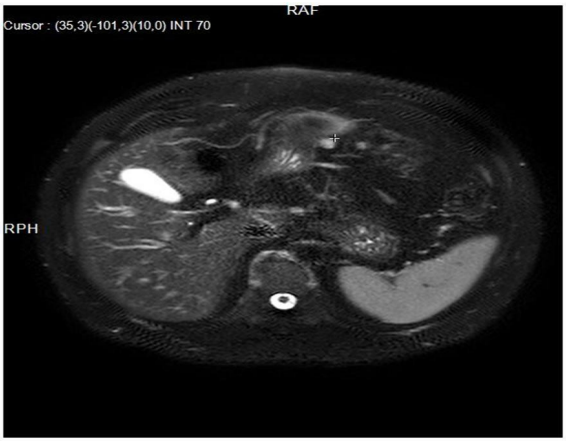

Fig. (2). GIST in the antrum of stomach, nodular hyperintense in the T2W-FS axial image with extraluminal positioning.

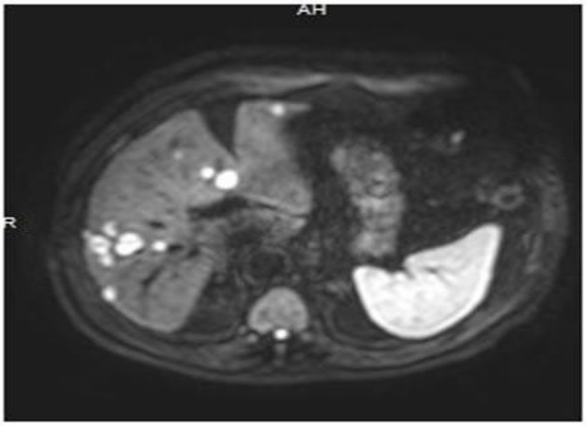

Fig. (3). Multiple hepatic metastasis of a GEP-NET with distinct diffusion restriction in the DWI.

* Address correspondence to this author at the Department of Radiology, İstanbul Medipol University, Pendik Education and Research Hospital, Adnan Menderes Bulvarı, Bahçelievler Mah. No:31/33 Pendik, İstanbul Tel: +90 505 466 35 34; E-mail: dr.hasanaydin@hotmail.com

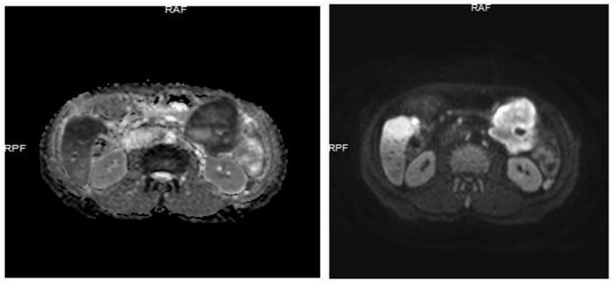

Fig. (4). A huge GIST located in the splenic flexura of colon, presenting a high diffusion restriction with very low ADC values and its hepatic metastasis in the right lobe of liver with similar diffusion restriction and hypointense signal amendments in ADC mapping.

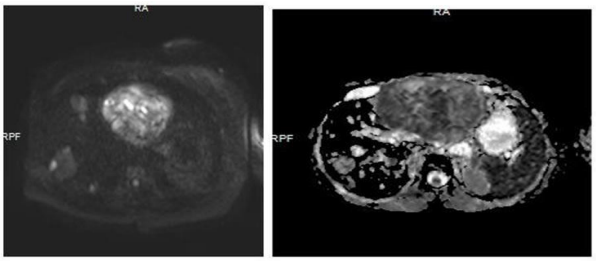

Fig. (5). A huge GIST in the stomach and its hepatic metastases, heterogeneous hyperintense in DWI hypointense in ADC mapping images, indicating a concrete diffusion restriction.

The elliptical or rectangular ROI's were placed on the solid-appearing and non-necrotic portions of pancreatic and hepatic masses by two experienced Abdominal radiologists. The hepatic segments which had occupied the metastatic lesions and their long diameters were also evaluated, all results were correlated with histopathology (Tables **4** and **5**). Parenchymal measurements obtained from the vascular structures were performed by inserting ROI and normal ADC values of normal liver *via* including 47 normal livers in the study. These values were measured as 1.20, ranging between 0.73-4.30 and compared with the average ADC values of metastasis (Table **6**). Those measurements were independent of the age and gender of the patients.

MR imaging was performed within 1,5 T MR units (32 mT/min gradient strength- Achieva; Philips Healthcare, Best, Netherlands and 32 channel GE Signa GE-Wisconsin-USA); by using a 4-8 channel standard phased-array torso XL coil. All images were evaluated by an Abdominal MRI experienced radiologist. DWI was performed in the transverse plane by using spin-echo-planar imaging sequence with the following parameters: TR/TE/inversion time: 12000/100/2200; diffusion gradient encoding in 3 orthogonal directions: b-0, b-400 ve b -800 s/mm^2. FOV: 385 mm; matrix size: 160-110 pixels; section thickness: 6 mm; section gap: 1 mm; and a number of signals acquired: 1. ADC measures were obtained from ADC mapping-by b value 800 s/mm^2. DWI scans were performed before contrast-enhanced T1-weighted imaging.

2.1. Statistics

For each continuous variable, Shapiro-Wilk Test of Normality was performed. Parametric or nonparametric analyses were applied depending on the distribution characteristics. Either Student's t test or Mann-Whitney U test was performed for the comparison of the two groups. When the group numbers were higher than two, One Way Analysis of Variance test or Kruskal Wallis Analysis of Variance test was performed. When pairwise comparisons were required, Tukey post hoc test or Mann Whitney U Test with Bonferroni Correction was applied. Data were shown as Mean ± Standard Deviation or Median (Min-Max) depending on the used method. In addition, Receiver Operating Characteristics (ROC) curve approach was used in order to characterize the group differences in terms of sensitivity, specificity, and positive and negative predictive value scores. Possible cut-off values were also interpreted with ROC curve analysis. For each statistical procedure, the level of significance (α) was accepted to be 0.05, p value <0.001 would indicate specific significant statistical differences (Graphic **1** and **2**).

Table 1. Mean age variations between GIST and GEP-NET patients.

-	Age	P
GIST (n=18)	57.18 ± 12.98	0.95
NET (n=12)	57.50 ± 15.52	

Table 2. Datas for primary GIST.

Localization	Diameter (mm)	ADC	Pathology
Duodenum- 2. part	18	1.22	Low Grade
Stomach -corpus	57	0.76	Intermediate
Colon Splenik Flexura	77	1.23	High grade
Pelvis	120	0.9	High grade
Terminal ileum	48	1.2	High grade
Mezentery	127	0.7	High grade
Stomach- cardia	28	0.7	Intermediate
Duodenum- 2. part	11	1.8	Low grade
Stomach- small curvature	50	1.4	Intermediate

(Table 2) contd.....

Stomach- small curvature	16	1.3	Low grade
Mesentery	30	0.62	Intermediate
Stomach- antrum	9	1.9	Low grade
Stomach- Pylor	30	0.28	Low grade
duodenum 2. part	12	0.96	Low grade
Stomach- great curvature	65	1.2	Intermediate
Jejenum	49	0.7	High grade
Mesentery	30	0.8	High grade
Mezentery	17	0.67	Intermediate

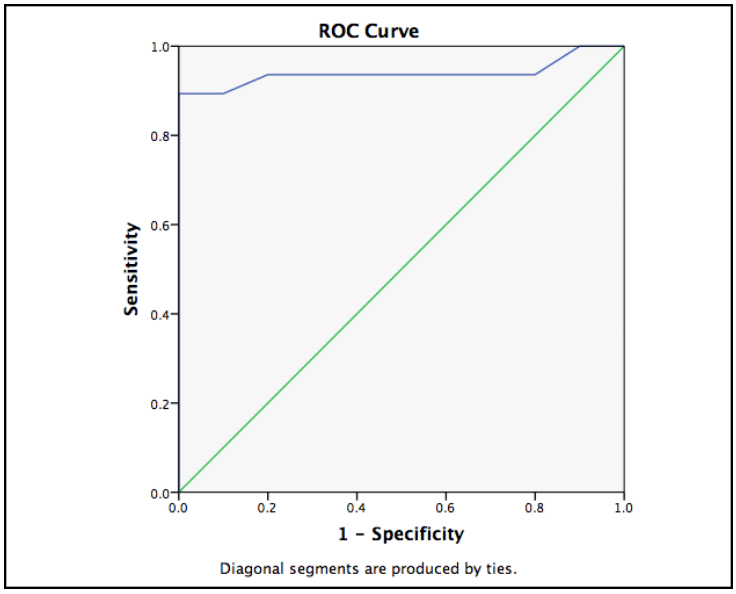

Graphic (1). ROC curve analysis of GIST_Liver _Met. (n=10) and normal liver(n:47) with regard to ADC values. Cut-off value for ADC: 0.925 Under AUC: 0.939 with 89.4% Sensitivity, 100% Specificity, 100% PPV and 66.7% PPV.

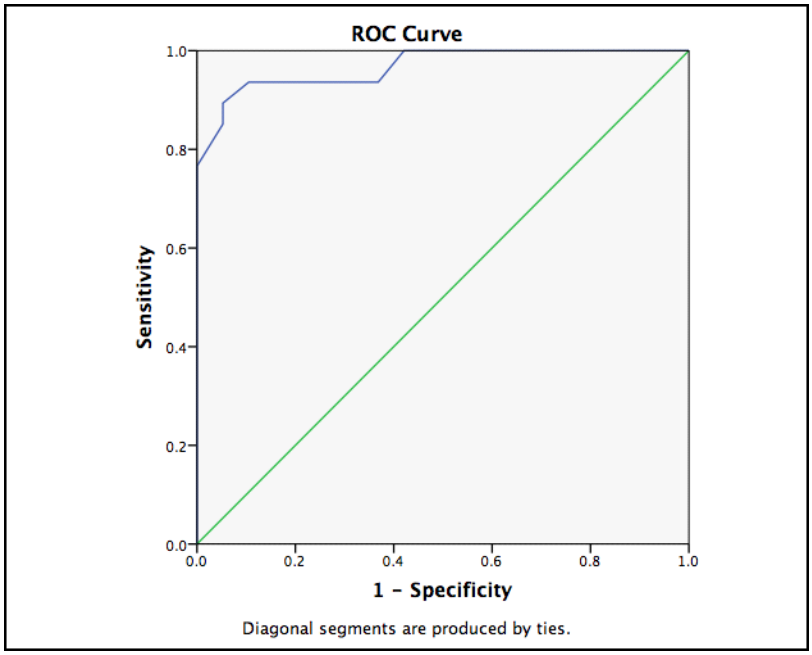

Graphic (2). ROC curve for ADC values between GEP NET_ Liver _Met (n=19) group and normal liver(n:47).Cut-off value for ADC: 0.860 under AUC: 0.967 with 93.6% Sensitivity, 89.5% Specificity, 95.7% PPV and 85% PPV.

Table 3. List of primary GEP-NETs.

Localization	Diameter (mm)	ADC	Pathology
Stomach	22mm	0.86	Well differentiated
Stomach	18mm	0.82	Well differentiated
Pelvis	68mm	0.84	Non-differentiated
Ampulla Watery	40mm	0.45	Large cell
Paraganglioma	38mm	0.78	Non-differentiated
Pancreas (insulinoma)	25mm	0.36	Non-differentiated
Paraganglioma seminal vezicles.	36mm	0.72	Non-differentiated
Paraganglioma	98mm	0.74	Non-differentiated

Table 4. Hepatic metastasis of GIST.

Localization	Diameter(mm)	ADC	Pathology
Segm 8	47mm	0.74	High grade
Segm 8	29mm	0.85	High grade
Segm 8	18mm	0.8	High grade
Segm 8	71mm	0.92	High grade
Segm 7	37mm	0.9	High grade
Segm 3	54mm	0.83	High grade
Segm 4	55mm	0.75	High grade
Segm 8	49mm	0.7	High grade
Segm 7	72mm	0.83	High grade
Segm 7	40mm	0.73	High grade
Segm 5	16mm	0.82	Well-differentiated
Segm 8	40mm	0.38-0.50	Un-differentiated.
Segm 7	50mm	0.42	Un-differentiated.
Segm 7	36mm	0.35	Un- differentiated.
segm 2	54mm	0.81	Un-differentiated.
Segm 4	40mm	0.55	Un-differentiated.
Segm 4	31mm	0.76	Un-differentiated.
Segm 4	63mm	0.75	Large cell
Seg 5	43mm	0.53	Large cell
Segm 6	33mm	0.61	large cell
Segm 5	5mm	0.28	Large cell
Segm 3	13mm	0.59	Large cell
Segm2	10mm	0.6	Large cell
Segm4	17mm	0.73	Un-differentiated.
Segm8	33mm	0.76	Un-differentiated.
Segm 6	20mm	0.67	Un-differentiated.
Segm 6	30mm	1	Un-differentiated.
Segm 5	15mm	0.9	Un-differentiated.
Seg 4	17mm	0.6	Un-differentiated.

Table 5. Hepatic metastasis of GEP-NET.

1.1	-							
1.1								
0.9	1.2	0.73	1.69	1.47	1.7	0.93	1.1	1.1
1.1	1.3	0.73	1.8	1.42	4.3	1.2	1.1	1.1
0.9	1	2.6	1.51	2.08	2.04	1	1.1	1.1
1.3	1	1,8	2.7	2.04	1.56	0.96	1.2	1.1
1.88	0.73	2.1	1.75	1.4	1.3	1	1.3	1.1

Table 6. Normal hepatic ADC values, non-dependant to age and gender of patients(s/mm^2).

-	Diameter	p	ADC	P
GIST (n=18)	30 (9-127)	0.72	0.93 (0.28-1.90)	0.13
GEP-NET (n=8)	37 (18-98)		0.76 (0.36-0.86)	

Table 7. Diameters and ADC values of GIST and GEP-NET patients, no significant statistical differences were observed.

-	ADC	P
GIST_Liver_Met.(n=10)	**0.82 (0.70-0.92) ***	**0.001**
GEP-NET_Liver_Met.(n=19)	**0.61 (0.28-1.00) +**	
Normal Liver(n=47)	**1.20 (0.73-4.30) Ω**	

Table 8. +: p=0.014. Correlation between GEP-NET_Liver_Met and GIST_Liver_Met.
p=0.001 Correlation between GIST_Liver_Met and normal control liver.
p=0.001 Comparison between GEP-NET_Liver_Met and normal control liver.

-	Diameter	P
GIST_KRC_MET (n=10)	48 (18-72)	0.016
NET_KRC_MET (n=19)	31 (5-63)	

Table 9. WHO Classification and Grading (2010) for GEP-NET.

WHO Classification and Grading (2010) for GEP-NET
•Well-differentiated neuroendocrine tumor (NET) (malignant behavior) –G1 – low grade <2% –G2 – intermediate grade 3%–19% • Information on individual value should be provided –G3 –high grade >20%
•Poorly differentiated neuroendocrine carcinoma (NEC) –G3 – high-grade malignant behavior >20 %

All statistical calculations and tests were performed with SPSS (Version 25.0) software.

In statistical analysis, both groups were correlated according to gender, ages, diameters of primary or metastatic masses, ADC values of them and segmental localizations of masses, in addition to those, ADC values of masses for both groups were compared to the normal ADC values of control liver group.

3. RESULTS

No statistical differences were observed between GIST and GEP-NET patients according to age and gender variations (Table **1**). Tables **2** and **3** present the localizations of GIST and GEP-NETs, their diameters-ADC values and pathologies. Diameter's of GIST's ranged between 9-127 mm; 30 mm average, ADC values ranged between 0.28-1.9; 0.93 average, pathologies were low to high grade. Diameter's of GEP-NET's ranged between 18-98 mm; 37 mm average, ADC values ranged between 0.36-0.86; 0.76 average, and pathologies were well to non-differentiated.

The majority of the localization of GIST metastasis was segment 8 (50%), segment 7 (30%) and segments 3 or 4, hepatic metastasis GEP-NET's were mostly located at segment 4 (26.3%). Diameter's of hepatic metastasis of GIST's ranged between 18-72 mm; 48 mm average, ADC values ranged between 0.70-0.92; 0.82 average, all had high-grade pathologies. Diameter's of hepatic metastasis of GEP-NET's ranged between 5-63 mm; 31 mm average, ADC values ranged between 0.28-1; 0.61 average, and pathologies ranged between well to undifferentiated (Tables **4** and **5**). In normal liver parenchyma, ADC values ranged between 0.73 to 4.30, 1.20 average (Table **6**).

No significant statistical differences were observed according to diameters and ADC values of GIST and GEP-NET patients (Table **7**). A significant statistical difference was observed between GIST and GEP-NET groups, in terms of the size of liver metastasis which was significantly higher in GIST patients.

All three groups (GIST_Hep. MET, GEP-NET_Liver_Met and normal) were statistically differed according to ADC values (Tables **8** and **9**).

With the ROC curve analysis: Hepatic metastasis of GIST(n=10) and normal liver (n:47) had cut-off value for ADC: 0.925 under AUC: 0.939 with regard to the ADC values

and regarded 89.4% Sensitivity, 100% Specificity, 100% PPV and 66.7% PPV. ROC curve of GEP NET_ Hepatic metastasis(n=19) group and normal liver(n:47) group presented a cut-off value for ADC: 0.860 under AUC: 0.967 correlated to the ADC values with 93.6% Sensitivity, 89.5% Specificity, 95.7% PPV and 85% PPV.

4. DISCUSSION

Liver is the most common site of metastasis after Lymph nodes, and hepatic metastasis may be single or multiple and occur in any segments [18, 19]. In this research, DWI and ADC values of liver metastasis of GIST and GEP-NET tumors were evaluated which were rarely seen gastrointestinal tumors [20 - 24].

DWI was mostly acquired in the diagnosis of ischemia, brain tumors and enfections [25 - 28]. It was more widely used in the remaining parts of the body, including liver, thyroid, prostate, musculoskeletal system, *etc*. [18, 19, 29 - 32]. At first, Muller *et al.* revealed the use of DWI in the differential diagnosis of liver, spleen, and musculoskeletal system disorders [29]. ADC value was also utilized in the evaluation and differential diagnosis of several disorders [30 - 33]. DWI has lots of advantages. A non-invasive approach without any ionizing radiation, no need to administer contrast agents, cheap and can be used in conjunction with conventional routine MR imaging [34, 35]. It mostly aids in the depiction of small sized lesions, mostly preferred in the diagnosis of liver metastasis, lower than 10 mm in size [18, 19, 36 - 38].

In recent reports, it was shown that DWI had great benefits in the detection of malignancy, metastasis and recurrence [25, 27, 34]. ADC value had reverse correlations to the tumoral cellularity, lower ADC values indicated hypercellularity and/or malignancy, Herneth *et al.* showed that tumors with high cellularity and higher density had high metastatic capacity [39]. In the literature, there were a few reports about the DWI of GIST, DWI and PET-CT were compared in those studies in which DWI had higher sensitivity [40, 41]. There were also a few reports about the diagnosis of GEP-NET by the application of DWI, predicting higher sensitivity of DWI in the detection and localization of metastatic GEP-NETs [8, 9, 13]; however, Artur *et al.* studied DWI and FSE T2, FFE T1W imaging after contrast enhancement and indicated that there was no significant difference between all three sequences [41].

GIST's are the most common mesenchymal tumor of the gastrointestinal tract and 1% of all gastrointestinal system tumors are mostly seen between 55-65 years of age without any gender predominance [1, 3, 5]. These tumors mostly arise from stomach (60%), then jejunum and ileum (30%), duodenum, rectum, esophagus and appendix are the least common sites of localizations, Omentum, retroperitoneum and mesentery are the extra-intestinal sites for the origin of GIST [1, 4, 6, 21]. GIST less than 5 cm in size are mostly discovered incidentally without any symptoms, characteristics of malignant GIST's are generally over 5 cm with heterogenous enhancement, lobulated-heterogenous contour and metastasis. The most common criteria is the tumor size and its mitotic index which are indicated by the grade of tumor [1, 3, 5, 6]. These tumors are classified as very low-low-moderate and high risk groups [2, 4 - 6, 20].

In our research, 7 stomach, 5 small intestine and mesentery, 1 colonic and pelvic GIST's were included as primary GIST. GIST tumors of the stomach did not present any high grade differentiation, but in the clinical follow-up, 2 high grade tumors had presented hepatic metastasis. In a patient, a hepatocellular carcinoma arose one year later without any symptoms of chronic liver diseases which was correlated with the relevant literature, indicating that GIST's might increase the incidence of other malignancies [2, 4, 5].

4.1. Risk Category of GIST

In the differential diagnosis of GIST, Mesenchymal tumors like Leiomyomas –leiomyosarcomas –schwannomas - neurofibromas and neuroendocrine tumors have to be considered, GIST's originating from both curvatures of the stomach have similar imaging findings with Gep-Net [1, 2, 6, 7].

Nowadays, PET-CT is a widely accepted imaging method in tumor grading and monitoring of treatment since it has a high sensitivity [33, 36, 42]. However, there are some disadvantages of PET-CT, including high radiation doses, the difficulties in its availability and preparing 18-fluorodeoxyglucose (FDG) for the patients, longer scanning time and high costs [33, 42]. Although DWI can be used as an alternative method to PET-CT since it is a radiation-free method, respiratory motion artifacts limit the image quality in DWI [30, 34, 35, 43 - 45]. In this research, ADC values for GIST metastasis had 89,4% sensitivity, 100% specificity and PPV, 66,7% NPV, these high and satisfactory results indicated DWI as an imaging modality of choice in the diagnosis of metastatic GIST [22, 39, 40].

GEP –NET's are the second most common gastrointestinal system tumors, % 1,2-1,5 of all gastrointestinal tumors, most common tumors of small intestine. Its prevalence in USA is higher than 100.000/year which is higher than the prevalence of stomach or pancreatic carcinoma [10 - 13, 15 - 17]. Neuroendocrine tumors of the stomach have an increasing incidence throughout the GEP-NET's, mostly seen at corpus of the stomach as small, polypoid, round, infiltrative and multifocal masses with 0.5-5 cm in size; these tumors usually do not generate any clinical symptoms [13 - 17].

Differentiations inside GEP-NET's varied according to their pathologies and hormonal syndromes caused by them. In 2010 WHO published a booklet dividing these tumors into neuroendocrine tumors and neuroendocrine carcinomas which could solve all suspicious problems between pathologists and clinicians [9, 13, 15, 16, 46]. In this classification, neuroendocrine tumors and neuroendocrine carcinomas are used as a nomenclature for GEP-NET's [13, 16, 17, 47]. Well-differentiated neuroendocrine tumors (NET) were benign without any malignant potentials, well-differentiated neuroendocrine carcinomas (NEC) revealed low-grade malignancy, poorly differentiated neuroendocrine carcinomas regarded high-grade malignant potentials [13, 16].

GEP-NET's are usually slowly growing tumors and 50% of them are non-metastatic and resectable when diagnosed [15 - 17, 25], but some subtypes had higher malignant and metastatic potentials, and grew faster [13, 16, 47]. Most

metastatic site was the liver which indicated poor prognosis [11, 13, 24]. In our study, only one well-differentiated GEP-NET had liver metastasis and the other 18 metastatic GEP-NET's were poorly-differentiated primary tumors. GEP-NET's have different clinical entities and prognoses, most of them are hypervascular and tri-phasic dynamic contrast-enhanced CT imaging with early-delayed arterial phases, portal venous phases are needed for accurate imaging and diagnosis, non-enhanced images show low-density and low accuracy in the detection of these lesions [11, 24].

<%5 of pancreatic NET's smaller than 1 cm in size were discovered by CT and MRI, whereas >%50 of these tumors over 3 cm in size were depicted by CT and MRI [10, 11, 25]. In this research, through the 19 GEP-NET metastasis diagnosed by DWI, 2 of them were less than 1 cm in size, 9 of them were less than 3 cm and these results were statistically higher than the conventional CT and MRI. Selective abdominal angiography was so sensitive in the diagnosis of pancreatic tail tumors [47]. In one patient, a diagnosis of GEP-NET that was located at pancreatic tail, was acquired by selective angiography.

Rockall *et al.* stated that diagnostic rate of hepatic metastasis was significantly increased by using liver specific contrast agents [48]. Herneth *et al.* reported that masses with higher cellularity and low ADC values had higher metastatic capacitie s [39]. Hayashida *et al.* indicated that the metastasis of undifferentiated adenoca had higher signal intensities than the other adenoca metastasis [27]. In some previous reports, it has been presented that ADC values of some focal liver lesions might be overlapping [30, 39, 49 - 53]. Tauli *et al.* also reported that metastatic masses had the lowest ADC values among hepatic masses [49]. Similar studies also indicated that ADC values were significantly lower in the other abdominal malignancies [39, 51, 54].

In this report, ADC values of GEP-NET's metastasis had 93,6% sensitivity and 89,5% specificity, GIST metastasis had 89,4% sensitivity and 100% specificity, against the ADC values of normal liver parenchyma. In this research, not only liver metastasis but conventional MR imaging and DWI of primary GIST and GEP-NET's were evaluated as well. ADC values of all these groups were compared to each other for primary GIST and GEP-NET's. Patient's age, gender, mass diameters and ADC values had no significant statistical differences.

Due to less number of cases and lack of classifications for mass localizations, further prospective researches with high number of cases are required. This is probably the major limitation of this research. Intravoxel incoherent motion and Diffusion Curtosis imaging with quantific numeric data may supplement valuable information in the discrimination of hepatic metastasis of GIST and GEP-NET's.

CONCLUSION

In most previous reports, it was reported that MRI was superior to CT in the diagnosis and follow-up of liver metastasis [38, 51 - 55]. DWI was a high MR imaging technique in the depiction of liver metastasis, and had superiority over CT and MRI in the detection of extrahepatic and extrapancreatic metastasis [18, 19, 31, 51, 53, 54]. In our research, high cellular tumors resulted from those liver metastases of GIST and GEP-NET's, a positive correlation was observed between ADC values and cellularity against differentiation ratios of metastatic masses. In the GIST group, cut-off ADC value was 0.925 for liver metastasis, whereas 0.860 for hepatic metastasis of GEP-NET's, both metastatic groups had higher sensitivity and specificity ratios.

ETHICS APPROVAL AND CONSENT TO PARTICIPATE

Ethics committee approval was not needed for this research because of its retrospective design in accordance with the opinions of Instutional Ethics Committee members.

HUMAN AND ANIMAL RIGHTS

No animal were used that are the basis of this study. Al the humans procedures were performed in accordance with the Helsinki declarations.

CONSENT FOR PUBLICATION

We had obtained consent for publication from the participants of this study.

STANDARDS OF REPORTING

STROBE guidelines were followed for this study.

AVAILABILITY OF DATA AND MATERIALS

Not applicable.

FUNDING

None

CONFLICT OF INTEREST

The authors declare no conflict of interest, financial or otherwise.

ACKNOWLEDGEMENTS

Declared none.

REFERENCES

[1] Aydin H, Metin MR, Kizilgoz V, *et al.* Results of gastrointestinal stromal tumors, correlated to the endoscopy-endosonography and histopathology. A retrospective research. J Cancer Clin Oncol 2015; 1(1): 100103.

[2] Grande C, Haller DG. Gastrointestinal stromal tumors and neuroendocrine tumors. Semin Oncol Nurs 2009; 25(1): 48-60. [http://dx.doi.org/10.1016/j.soncn.2008.10.004] [PMID: 19217505]

[3] Miettinen M, Lasota J. Gastrointestinal stromal tumors-Definition, clinical, histological, immunohistochemical, and molecular genetic features and differential diagnosis. Virchows Arch 2001; 438(1): 1-12. [http://dx.doi.org/10.1007/s004280000338] [PMID: 11213830]

[4] Horwitz BM, Zamora GE, Gallegos MP. Best cases from the AFIP: Gastrointestinal stromal tumor of the small bowel. Radiographics 2011; 31(2): 429-34. [http://dx.doi.org/10.1148/rg.312105031] [PMID: 21415188]

[5] Bareck E, Ba-Ssalamah A, Brodowicz T, *et al.* Gastrointestinal stromal tumors: Diagnosis, therapy and follow-up care in Austria. Wien Med Wochenschr 2013; 163(5-6): 137-52. [http://dx.doi.org/10.1007/s10354-013-0187-3] [PMID: 23508516]

[6] Kim HC, Lee JM, Kim KW, *et al.* Gastrointestinal stromal tumors of the stomach: CT findings and prediction of malignancy. AJR Am J

Roentgenol 2004; 183(4): 893-8.
[http://dx.doi.org/10.2214/ajr.183.4.1830893] [PMID: 15385278]

[7] Sundin A, Vullierme MP, Kaltsas G, Plöckinger U. ENETS consensus guidelines for the standards of care in neuroendocrine tumors: Radiological examinations. Neuroendocrinology 2009; 90(2): 167-83.
[http://dx.doi.org/10.1159/000184855] [PMID: 19077417]

[8] Kulali F, Semiz-Oysu A, Demir M, Segmen-Yilmaz M, Bukte Y. Role of diffusion-weighted MR imaging in predicting the grade of nonfunctional pancreatic neuroendocrine tumors. Diagn Interv Imaging 2018; 99(5): 301-9.
[http://dx.doi.org/10.1016/j.diii.2017.10.012] [PMID: 29258825]

[9] Verde F, Galatola R, Romeo V, *et al.* Pancreatic neuroendocrine tumors in patients with multiple endocrine neoplasia type 1: Diagnostic value of different MRI sequences. Neuroendocrinology 2021; 111: 696-704.
[http://dx.doi.org/10.1159/000509647]

[10] Leung D, Schwartz L. Imaging of neuroendocrine tumors. Semin Oncol 2013; 40(1): 109-19.
[http://dx.doi.org/10.1053/j.seminoncol.2012.11.008] [PMID: 23391118]

[11] Rockall AG, Reznek RH. Imaging of neuroendocrine tumours (CT/MR/US). Best Pract Res Clin Endocrinol Metab 2007; 21(1): 43-68.
[http://dx.doi.org/10.1016/j.beem.2007.01.003] [PMID: 17382265]

[12] Plöckinger U, Rindi G, Arnold R, *et al.* Guidelines for the diagnosis and treatment of neuroendocrine gastrointestinal tumours. A consensus statement on behalf of the European Neuroendocrine Tumour Society (ENETS). Neuroendocrinology 2004; 80(6): 394-424.
[http://dx.doi.org/10.1159/000085237] [PMID: 15838182]

[13] McDermott S, O'Neill AC, Skehan SJ. Staging of gastroenteropancreatic neuroendocrine tumors: How we do it based on an evidence-based approach. Clin Imaging 2013; 37(2): 194-200.
[http://dx.doi.org/10.1016/j.clinimag.2012.05.006] [PMID: 23465968]

[14] Bonds M, Rocha FG. Neuroendocrine tumors of the pancreatobiliary and gastrointestinal tracts. Surg Clin North Am 2020; 100(3): 635-48.
[http://dx.doi.org/10.1016/j.suc.2020.02.010] [PMID: 32402306]

[15] Eriksson B, Kloeppel G, Krenning EP, *et al.* Consensus guidelines for the management of patients with digestive neuroendocrine tumors-well-differentiated jejunal-ileal tumor/carcinoma. Neuroendocrinology 2008; 87: 8-19.
[http://dx.doi.org/https://doi.org/10.1159/000111034]

[16] Öberg K, Astrup L, Eriksson B, *et al.* Guidelines for the management of gastroenteropancreatic neuroendocrine tumours (including bronchopulmonary and thymic neoplasms). Acta Oncol 2004; 43(7): 616.
[http://dx.doi.org/10.1080/02841860410018502] [PMID: 15545182]

[17] Cives M, Strosberg JR. Gastroenteropancreatic neuroendocrine tumors. CA Cancer J Clin 2018; 68(6): 471-87.
[http://dx.doi.org/10.3322/caac.21493] [PMID: 30295930]

[18] Namimoto T, Yamashita Y, Sumi S, Tang Y, Takahashi M. Focal liver masses: characterization with diffusion-weighted echo-planar MR imaging. Radiology 1997; 204(3): 739-44.
[http://dx.doi.org/10.1148/radiology.204.3.9280252] [PMID: 9280252]

[19] Ichikawa T, Haradome H, Hachiya J, Nitatori T, Araki T. Diffusion-weighted MR imaging with a single-shot echoplanar sequence: Detection and characterization of focal hepatic lesions. AJR Am J Roentgenol 1998; 170(2): 397-402.
[http://dx.doi.org/10.2214/ajr.170.2.9456953] [PMID: 9456953]

[20] Bano S, Puri SK, Upreti L, Chaudhary V, Sant HK, Gondal R. Gastrointestinal stromal tumors (GISTs): An imaging perspective. Jpn J Radiol 2012; 30(2): 105-15.
[http://dx.doi.org/10.1007/s11604-011-0020-0] [PMID: 22190071]

[21] Burkill GJC, Badran M, Al-Muderis O, *et al.* Malignant gastrointestinal stromal tumor: Distribution, imaging features, and pattern of metastatic spread. Radiology 2003; 226(2): 527-32.
[http://dx.doi.org/10.1148/radiol.2262011880] [PMID: 12563150]

[22] Ulusan S, Koç Z. Radiologic findings in malignant gastrointestinal stromal tumors. Diagn Interv Radiol 2009; 15(2): 121-6.
[PMID: 19517382]

[23] Werewka-Maczuga A, Osiński T, Chrzan R, Buczek M, Urbanik A. Characteristics of computed tomography imaging of gastrointestinal stromal tumor (GIST) and related diagnostic problems. Pol J Radiol 2011; 76(3): 38-48.
[PMID: 22802840]

[24] Taal BG, Visser O. Epidemiology of neuroendocrine tumours. Neuroendocrinology 2004; 80(Suppl. 1): 3-7.
[http://dx.doi.org/10.1159/000080731] [PMID: 15477707]

[25] Yao JC, Hassan M, Phan A, *et al.* One hundred years after "carcinoid": Epidemiology of and prognostic factors for neuroendocrine tumors in 35,825 cases in the United States. J Clin Oncol 2008; 26(18): 3063-72.
[http://dx.doi.org/10.1200/JCO.2007.15.4377] [PMID: 18565894]

[26] Guo AC, Cummings TJ, Dash RC, Provenzale JM. Lymphomas and high-grade astrocytomas: Comparison of water diffusibility and histologic characteristics. Radiology 2002; 224(1): 177-83.
[http://dx.doi.org/10.1148/radiol.2241010637] [PMID: 12091680]

[27] Hayashida Y, Hirai T, Morishita S, *et al.* Diffusion-weighted imaging of metastatic brain tumors: Comparison with histologic type and tumor cellularity. AJNR Am J Neuroradiol 2006; 27(7): 1419-25.
[PMID: 16908550]

[28] Sugita R, Yamazaki T, Furuta A, Itoh K, Fujita N, Takahashi S. High b-value diffusion-weighted MRI for detecting gallbladder carcinoma: Preliminary study and results. Eur Radiol 2009; 19(7): 1794-8.
[http://dx.doi.org/10.1007/s00330-009-1322-9] [PMID: 19190910]

[29] Müller MF, Prasad P, Siewert B, Nissenbaum MA, Raptopoulos V, Edelman RR. Abdominal diffusion mapping with use of a whole-body echo-planar system. Radiology 1994; 190(2): 475-8.
[http://dx.doi.org/10.1148/radiology.190.2.8284402] [PMID: 8284402]

[30] Kwee TC, Takahara T, Ochiai R, *et al.* Whole-body diffusion-weighted magnetic resonance imaging. Eur J Radiol 2009; 70(3): 409-17.
[http://dx.doi.org/10.1016/j.ejrad.2009.03.054] [PMID: 19403255]

[31] Kim T, Murakami T, Takahashi S, Hori M, Tsuda K, Nakamura H. Diffusion-weighted single-shot echoplanar MR imaging for liver disease. AJR Am J Roentgenol 1999; 173(2): 393-8.
[http://dx.doi.org/10.2214/ajr.173.2.10430143] [PMID: 10430143]

[32] Ries M, Jones RA, Basseau F, Moonen CTW, Grenier N. Diffusion tensor MRI of the human kidney. J Magn Reson Imaging 2001; 14(1): 42-9.
[http://dx.doi.org/10.1002/jmri.1149] [PMID: 11436213]

[33] Wong CS, Gong N, Chu YC, *et al.* Correlation of measurements from diffusion weighted MR imaging and FDG PET/CT in GIST patients: ADC *versus* SUV. Eur J Radiol 2012; 81(9): 2122-6.
[http://dx.doi.org/10.1016/j.ejrad.2011.09.003] [PMID: 21955604]

[34] Charles-Edwards EM, deSouza NM. Diffusion-weighted magnetic resonance imaging and its application to cancer. Cancer Imaging 2006; 6(1): 135-43.
[http://dx.doi.org/10.1102/1470-7330.2006.0021] [PMID: 17015238]

[35] Bammer R. Basic principles of diffusion-weighted imaging. Eur J Radiol 2003; 45(3): 169-84.
[http://dx.doi.org/10.1016/S0720-048X(02)00303-0] [PMID: 12595101]

[36] Gourtsoyianni S, Papanikolaou N, Yarmenitis S, Maris T, Karantanas A, Gourtsoyiannis N. Respiratory gated diffusion-weighted imaging of the liver: value of apparent diffusion coefficient measurements in the differentiation between most commonly encountered benign and malignant focal liver lesions. Eur Radiol 2008; 18(3): 486-92.
[http://dx.doi.org/10.1007/s00330-007-0798-4] [PMID: 17994317]

[37] Lestra T, Kanagaratnam L, Mulé S, *et al.* Measurement variability of liver metastases from neuroendocrine tumors on different magnetic resonance imaging sequences. Diagn Interv Imaging 2018; 99(2): 73-81.
[http://dx.doi.org/10.1016/j.diii.2017.12.009] [PMID: 29339222]

[38] Quan XY, Sun XJ, Yu ZJ, Tang M. Evaluation of diffusion weighted imaging of magnetic resonance imaging in small focal hepatic lesions: a quantitative study in 56 cases. Hepatobiliary Pancreat Dis Int 2005; 4(3): 406-9.
[PMID: 16109526]

[39] Herneth AM, Guccione S, Bednarski M. Apparent Diffusion Coefficient: a quantitative parameter for in vivo tumor characterization. Eur J Radiol 2003; 45(3): 208-13.
[http://dx.doi.org/10.1016/S0720-048X(02)00310-8] [PMID: 12595105]

[40] Gong NJ, Wong CS, Chu YC, Gu J. Treatment response monitoring in patients with gastrointestinal stromal tumor using diffusion-weighted imaging: preliminary results in comparison with positron emission tomography/computed tomography. NMR Biomed 2013; 26(2): 185-92.
[http://dx.doi.org/10.1002/nbm.2834] [PMID: 22806958]

[41] Sankowski AJ, Ćwikla JB, Nowicki ML, *et al.* The clinical value of MRI using single-shot echoplanar DWI to identify liver involvement in patients with advanced gastroenteropancreatic-neuroendocrine tumors (GEP-NETs), compared to FSE T2 and FFE T1 weighted image after i.v. Gd-EOB-DTPA contrast enhancement. Med Sci Monit 2012; 18(5): MT33-40.

[http://dx.doi.org/10.12659/MSM.882719] [PMID: 22534718]

[42] Lordick F, Ott K, Krause BJ, *et al.* PET to assess early metabolic response and to guide treatment of adenocarcinoma of the oesophagogastric junction: The MUNICON phase II trial. Lancet Oncol 2007; 8(9): 797-805. [http://dx.doi.org/10.1016/S1470-2045(07)70244-9] [PMID: 17693134]

[43] Ivancevic MK, Kwee TC, Takahara T, *et al.* Diffusion-weighted MR imaging of the liver at 3.0 Tesla using TRacking Only Navigator echo (TRON): A feasibility study. J Magn Reson Imaging 2009; 30(5): 1027-33. [http://dx.doi.org/10.1002/jmri.21939] [PMID: 19856431]

[44] Nemeth AJ, Henson JW, Mullins ME, Gonzalez RG, Schaefer PW. Improved detection of skull metastasis with diffusion-weighted MR imaging. AJNR Am J Neuroradiol 2007; 28(6): 1088-92. [http://dx.doi.org/10.3174/ajnr.A0501] [PMID: 17569964]

[45] Cossetti RJD, Bezerra ROF, Gumz B, Telles A, Costa FP, Frederico PC. Whole body diffusion for metastatic disease assessment in neuroendocrine carcinomas: comparison with OctreoScan® in two cases. World J Surg Oncol 2012; 10(1): 82. [http://dx.doi.org/10.1186/1477-7819-10-82] [PMID: 22591909]

[46] Caplin ME, Buscombe JR, Hilson AJ, Jones AL, Watkinson AF, Burroughs AK. Carcinoid tumour. Lancet 1998; 352(9130): 799-805. [http://dx.doi.org/10.1016/S0140-6736(98)02286-7] [PMID: 9737302]

[47] Jackson JE. Angiography and arterial stimulation venous sampling in the localization of pancreatic neuroendocrine tumours. Best Pract Res Clin Endocrinol Metab 2005; 19(2): 229-39. [http://dx.doi.org/10.1016/j.beem.2004.10.002] [PMID: 15763697]

[48] Rockall AG, Planche K, Power N, *et al.* Detection of neuroendocrine liver metastases with MnDPDP-enhanced MRI. Neuroendocrinology 2009; 89(3): 288-95. [http://dx.doi.org/10.1159/000176207] [PMID: 19023191]

[49] Taouli B, Vilgrain V, Dumont E, Daire JL, Fan B, Menu Y. Evaluation of liver diffusion isotropy and characterization of focal hepatic lesions with two single-shot echo-planar MR imaging sequences: prospective study in 66 patients. Radiology 2003; 226(1): 71-8. [http://dx.doi.org/10.1148/radiol.2261011904] [PMID: 12511671]

[50] Ståhlberg F, Brockstedt S, Thomsen C, Wirestam R. Single-shot diffusion-weighted echo-planar imaging of normal and cirrhotic livers using a phased-array multicoil. Acta Radiol 1999; 40(3): 339. [PMID: 10335977]

[51] Parikh T, Drew SJ, Lee VS, Wong S, Hecht EM, Babb JS, *et al.* Focal liver lesions detection and characterization with Diffusion MR Imaging: Comparison with breath hold T2 weighted imaging. Radiology 2008; 246: 812-22. [http://dx.doi.org/10.1148/radiol.2463070432] [PMID: 18223123]

[52] Anadol N. Karaciğer lezyonlarının benign malign ayrımında PET benzeri kontrasta sahip MR difüzyon görüntülerinin değeri. 2016. Available from: http://abakus.inonu.edu.tr/xmlui/bitstream/handle/11616/9781/431673.pdf?sequence=1

[53] Nasu K, Kuroki Y, Nawano S, *et al.* Hepatic metastases: diffusion-weighted sensitivity-encoding versus SPIO-enhanced MR imaging. Radiology 2006; 239(1): 122-30. [http://dx.doi.org/10.1148/radiol.2383041384] [PMID: 16493012]

[54] Danet IM, Semelka RC, Leonardou P, *et al.* Spectrum of MRI appearances of untreated metastases of the liver. AJR Am J Roentgenol 2003; 181(3): 809-17. [http://dx.doi.org/10.2214/ajr.181.3.1810809] [PMID: 12933487]

[55] Noone TC, Hosey J, Firat Z, Semelka RC. Imaging and localization of islet-cell tumours of the pancreas on CT and MRI. Best Pract Res Clin Endocrinol Metab 2005; 19(2): 195-211. [http://dx.doi.org/10.1016/j.beem.2004.11.013] [PMID: 15763695]